

Investigation of negative BOLD responses in human brain through NIRS technique. A visual stimulation study

Eleonora Maggioni ^{a,b,*}, Erika Molteni ^b, Claudio Zucca ^b, Gianluigi Reni ^b, Sergio Cerutti ^a, Fabio M. Triulzi ^{b,c}, Filippo Arrigoni ^b, Anna M. Bianchi ^a

^a Department of Electronics, Information and Bioengineering, Politecnico di Milano, Milano, Italy

^b Scientific Institute IRCCS E.Medea, Bosisio Parini, Lecco, Italy

^c Neuroradiology Unit, Fondazione IRCCS Cà Granda, Ospedale Maggiore Policlinico, Milano, Italy

Accepted 29 December 2014

Available online 8 January 2015

Introduction

Functional magnetic resonance imaging (fMRI) has been largely used to gain insight into human visual cortical function. Most studies focus on functional activation and look for positive BOLD responses to visual stimuli, which are known to be coupled to neuronal activity (Ogawa et al., 1990; Logothetis et al., 2001). However, increasing interest is being given by negative BOLD responses (NBRs), *i.e.* BOLD decreases below baseline, which were observed in cerebral areas different from the primary visual cortex and whose origin is less straightforward to characterize.

NBRs to visual tasks have been reported in both animals and humans (Shmuel et al., 2002; Smith et al., 2004; Bressler et al., 2007; Goense et al., 2012). Such responses, however, are not peculiar to the visual

system, since they have been shown to occur in response to somatosensory stimuli (Devor et al., 2007; Kastrup et al., 2008; Schäfer et al., 2012) and in the motor cortex (Hamzei et al., 2002; Stefanovic et al., 2004).

In a recent study on healthy subjects, spatially inhomogeneous fMRI responses to intermittent photic stimulation (IPS) were observed. Preliminary results from Arrigoni et al. (2013) and Maggioni et al. (2013) showed a complex pattern of positive and negative BOLD changes, involving both striate and extra-striate visual cortexes during IPS. In addition to the positive BOLD response (PBR) in the primary visual cortex, two symmetric regions with significant NBR were detected, located in the inferior portion of the lateral occipital cortex (LOC) (Larsson and Heeger, 2006). The NBRs to IPS are more extended and exhibit higher amplitude compared to previously described visual NBRs (Shmuel et al., 2002; Bressler et al., 2007; Goense et al., 2012). A further difference *versus* previous studies concerns the location of the NBRs. The spatial extension of these NBRs and their high amplitude, which was comparable to the PBR one, increased the interest towards the underlying neuronal, metabolic and vascular mechanisms.

Despite many efforts made towards a better comprehension of the negative BOLD phenomenon, its origin is still under discussion. Some studies suggested that the NBR could be related to a hemodynamic

* Corresponding author at: Department of Electronics, Information and Bioengineering (DEIB), Politecnico di Milano, Via C. Golgi, 39, 20133 Milan (MI), Italy. Fax: +39 0223993360.

E-mail addresses: eleonora.maggioni@polimi.it, emaggioni@bp.inf.it (E. Maggioni).

effect (Shmuel et al., 2002), but currently the most acknowledged theory is that the NBR is neuronal in origin (Smith et al., 2004; Bressler et al., 2007; Pasley et al., 2007; Mullinger et al., 2014).

There are further controversial interpretations of NBR determinants. In fact, the BOLD signal arises from a complex coupling between cerebral blood flow (CBF), cerebral blood volume (CBV) and cerebral metabolic rate of oxygen consumption (CMRO₂), thus making it difficult to identify their exact contributions to the NBR phenomenon.

Multimodal imaging is a powerful tool to this effect, as it provides additional measurements that can help shed light on the factors underlying NBR. Up until now, BOLD measurements have been combined with electrophysiological recordings in order to unveil the associated neurovascular coupling (Mullinger et al., 2014), while measures of CBV and CBF helped understand the direct determinants of NBRs (Goense et al., 2012; Huber et al., 2014). A common finding is that NBRs are associated to a decrease in CBF (Shmuel et al., 2002; Stefanovic et al., 2004; Pasley et al., 2007; Schäfer et al., 2012; Mullinger et al., 2014), although a full hemodynamic characterization of this phenomenon is still lacking.

In the present paper we focus on the hemodynamic and metabolic aspects related to the cerebral response to IPS. The main scientific question under investigation is: what are the vascular underpinnings of negative BOLD responses to IPS? In this view, we associated the fMRI observations to optical measurements, which can provide more exact information on oxygen concentration and CBF.

In point of fact, optical techniques, such as near infrared spectroscopy (NIRS), may be employed to obtain a more complete understanding of NBRs. Thanks to its biochemical specificity, NIRS measures the changes in oxyhemoglobin (HbO) and deoxyhemoglobin (HHb) concentrations with a good temporal resolution (up to 0.1 s), at the detriment of a spatial resolution of the order of centimeters. Despite many NIRS studies on visual stimulations have been performed (Kato et al., 1993; Gratton et al., 2001; Jaszewski et al., 2003; Plichta et al., 2007), only a few combined NIRS with fMRI technique (Schroeter et al., 2006; Toronov et al., 2006). At present, the only study that identified NBRs in the visual cortex with both fMRI and NIRS was carried out by (Moosmann et al., 2003), but did not perform an in-depth analysis of the NBR characteristics.

The present study follows a preliminary analysis of (Maggioni et al., 2013) and aims to gain insight into the properties of NBRs to IPS by combining fMRI and NIRS findings. The information provided by NIRS about the temporal evolution of blood oxygenation can be a key factor for a thorough understanding of the negative BOLD phenomenon. Although acquired in separate sessions, we compared fMRI and NIRS data by hypothesizing that visual stimulation provokes the same average response across multiple acquisitions.

First, the results of the fMRI activation analysis were compared to the NIRS findings; then, after extracting the BOLD signal corresponding to the voxels underlying each NIRS channel, the association between negative BOLD and the corresponding Hb signals was studied. In particular, we analyzed and compared the BOLD and the NIRS time series extracted from the same cortical areas, in order to 1) define which hemoglobin species is mostly correlated with the BOLD trend, 2) estimate possible differences in response time between the two modalities and 3) estimate possible differences in the dynamical response in the two modalities.

Materials and methods

Experimental protocol

The experimental procedure and acquisition parameters that are described hereinafter are the same as in Maggioni et al. (2013).

Subjects

Eight healthy volunteers (3 males, 5 females, mean age 27.9 years, standard deviation 3.39 years) participated in this study. All of them had normal vision and no history of epileptic seizures or any other neurological or vascular pathology. The protocol was approved by the Ethic Committee of IRCCS E. Medea – Associazione “La Nostra Famiglia” and informed written consent was obtained from each subject after a discussion of the aim and the procedures of the study.

Visual stimulation procedure

The stimulation protocol was developed with the Presentation® software (Neurobehavioral Systems Inc.). A block-designed IPS was created by reversing black and white screens at four different frequencies (6, 8, 10 and 12 Hz) in a progressive order of presentation. Rest epochs lasting 14 s (corresponding to 7 scans for the MRI sequence and 111 samplings for the NIRS recording) were alternated with same length stimulation epochs. This duration was long enough to allow for the exhaustion of IPS response from one IPS block to another. Five blocks for each stimulation frequency were included. Subjects were asked to keep their eyes open throughout the experiment; during rest periods, they were asked to look at a yellow fixation cross in the center of a black background. Each frequency block was repeated five times during fMRI acquisition and eight times during NIRS acquisition in order to obtain an adequate signal to noise ratio (SNR). The total duration of the fMRI and NIRS experiments was 594 s (including dummy scans) and 928 s, respectively. The fMRI and NIRS sessions took place on two different days; in the two sessions, two structural MRI acquisitions were performed for coregistration purposes.

fMRI data acquisition

All MR scans were acquired with a 3 Tesla scanner (Philips Achieva, Best, The Netherlands), equipped with a 32-channel head coil. Within the MRI experiment, an anatomical T1-weighted 3D Turbo Field Echo (TFE) sequence was run for morphological referencing of MRI data, with the parameters set as follows: 1 mm isotropic resolution, field of view (FOV) = 240 × 240 × 175 mm³, repetition time (TR) = 8.19 ms, echo time (TE) = 3.74 ms, and flip angle = 8°. fMRI data were acquired with a T2*-weighted gradient-echo planar sequence (TR = 2 s, TE = 35 ms, flip angle = 85°, 30 axial slices without gap, FOV = 240 × 105 × 240 mm³, voxel size = 1.875 × 1.875 × 3.5 mm³) covering the cerebral hemispheres, with the exclusion of the cerebellum and brainstem. Visual stimuli were delivered in the MR scanner through MRI-compatible goggles (Resonance Technology Inc.).

NIRS data acquisition and optode localization

A commercial continuous wave NIRS device (DYNOT Compact, NIRx Berlin) was employed for NIRS recordings. An elastic cap of proper head size was fitted on the subjects' head. The cap had been previously tailored for a bilateral 16-channel montage, centered over the bilateral parieto-occipital brain area. NIRS recordings were performed at two different wavelengths (760 nm and 830 nm), in order to selectively probe oxygenated and deoxygenated hemoglobin species (HbO and HHb respectively) in the brain. The visual stimulation was shown on a computer screen.

After each NIRS recording, a structural MR image of the subject was acquired to provide a spatial prior for NIRS and to identify the position of emitters and detectors. Localization was performed after removal of the optical probes by attaching vitamin E pills (showing bright signals on T1-weighted MR sequences) to the NIRS cap in place of each probe. We used a T1-weighted 3D TFE sequence (1 mm isotropic resolution, FOV = 240 × 240 × 175 mm³, TR = 8.13 ms, TE = 3.73 ms, flip angle = 8°) identical to the one used during fMRI acquisition.

Data analysis

General linear model activation analysis

fMRI data processing. The fMRI data of each subject were processed with the statistical parametric mapping (SPM) software (<http://www.fil.ion.ucl.ac.uk/spm/>, version 8) (Friston et al., 2011). Pre-processing included spatial realignment to reduce head motion artifacts, coregistration of the mean functional image to the structural images, normalization to the MNI template (only for group analysis) and spatial smoothing with a 3D Gaussian kernel filter with a full half width maximum (FWHM) of 6 mm³. Each IPS block was convolved with the canonical hemodynamic response function (HRF) (Friston et al., 2011) and was then used as regressor. Pre-processed fMRI data in native space were used for single-subject analysis; in addition, we used pre-processed fMRI data in MNI space in a fixed-effect group GLM analysis using a unique design matrix including the eight subjects and all tasks (Beckmann et al., 2003). In both analyses, the effects of IPS compared to rest conditions were assessed by inference with a two-sided t-test. Since the different frequencies of stimulation produced similar effects on the BOLD signal (without significant differences), the IPS frequencies were analyzed all together. The coordinates of significant regions of the group analysis were saved with the SPM MarsBar toolbox (<http://marsbar.sourceforge.net/>) (Brett et al., 2002). We then used the GMAC toolbox (<http://selene.bioing.polimi.it/BBBlab/GMAC>) (Tana et al., 2012) to extract the pre-processed BOLD time series corresponding to each ROI from all subjects. The BOLD time series were extracted after removal of the nuisance variables, *i.e.* the remaining sources of spurious variance (Tana et al., 2012). A session-specific grand mean scaling was used to set the mean value of the intracerebral voxels over space and time (within a session) to 100. This allowed interpreting the BOLD signal change as percent of the global intracerebral mean (Friston et al., 2011). The resulting curves were then inspected and temporal and amplitude parameters were calculated.

NIRS data processing. NIRS data were visually inspected for artifact removal and then filtered with a low-pass filter at 0.3 Hz. Continuous tracks were then segmented into epochs starting at the beginning of each IPS block and ending at the end of the following rest block. In so doing, we extracted 32 epochs, each one lasting 28 s, which were grouped for single-subject average. For each subject, a GLM was estimated by using as regressor the IPS blocks convolved with the canonical HRF, as in the fMRI analysis. A two-sided t-test was then used for inference of the IPS effects. We only performed the analysis at a single-subject level, because the position variability of the NIRS channels between subjects precluded the group analysis.

Spatial coregistration between NIRS and fMRI data

The Freesurfer software (<http://surfer.nmr.mgh.harvard.edu>) (Dale et al., 1999) was used for a 3D reconstruction of the native cortical surface of each subject, starting from the structural MR image. The fMRI statistical map in native space resulting from single-subject GLM analysis was co-registered and represented on the pial surface of one exemplar subject.

The position of the NIRS optodes on the scalp was identified by using vitamin E markers and the coordinates of each NIRS channel were estimated as the midpoint between the corresponding source and detector. Then, Freesurfer was used to project the NIRS channel coordinates on the reconstructed pial surface.

fMRI–NIRS signals comparison

The BOLD versus Hb comparison was performed using the single-subject NIRS and fMRI data. An outline of the fMRI–NIRS comparison in each subject is shown in Fig. 1.

NIRS data pre-processing. Before comparison with BOLD signals, the NIRS raw data of each channel and subject were pre-processed in order to reduce any global interference. After removing the signal mean from the entire signal, we extracted 28 s epochs, each one corresponding to one IPS block and the following rest block. A linear detrend was applied to each epoch. Taking the mean of the maximum amplitudes across the different epochs as reference, we discarded the epochs having a maximum value higher than the double. The accepted epochs were finally averaged, resulting in one representative IPS response for each channel.

fMRI data pre-processing and extraction. To compare fMRI and NIRS time series, we extracted the mean BOLD signal corresponding to the fMRI voxels underlying each NIRS recording site. In this way, we obtained one BOLD fMRI time series relative to each NIRS time series. The path of the photons from the emitter to the detector was approximated to a half circle and we took the NIRS sensitivity region as a 1 cm radius semi-sphere centered on the projection of the NIRS channel over the pial surface. The SPM Marsbar toolbox was used to define the spherical regions of interest (ROIs); we then extracted the mean BOLD signal of the fMRI voxels corresponding to the semi-sphere within the brain mask. As in the group fMRI analysis, the extraction of raw fMRI time series was performed using the pre-processed fMRI images with the GMAC toolbox, after removal of the nuisance variables (Tana et al., 2012) and session-specific grand mean scaling (Friston et al., 2011).

Effect size of NIRS and fMRI data. After pre-processing, the size of the IPS effect on NIRS and fMRI data was estimated to provide a measure of contrast to noise ratio (CNR). For each NIRS channel, the effect size d (Cohen, 1992) was calculated using the following formula

$$d = \frac{|(\text{mean}(\text{IPS}) - \text{mean}(\text{rest}))|}{\sqrt{((N1-1) * \text{std}(\text{IPS})^2 + (N2-1) * \text{std}(\text{rest})^2) / (N1 + N2 - 2)}} \quad (1)$$

where the absolute difference between the mean signal amplitude during IPS (from 6 s to the end of the IPS blocks) and rest blocks (from 6 s to the end of rest blocks) was divided for the pooled standard deviation ($N1$ and $N2$ are the number of samples in IPS and rest blocks respectively). We did not consider the first seconds of IPS and rest blocks in order to discard the ascent and descent of the hemodynamic response. For each NIRS channel, the values of effect size of HbO, Hb and BOLD signals in the group were compared through a Kruskal–Wallis test; if significant differences emerged between the three species ($p < 0.01$), a pairwise comparison was performed. It needs to be mentioned that this channel-wise comparison could be limited by the different position of NIRS channels from subject to subject. To provide a global measure of task-related SNR of NIRS and fMRI data, we computed the median value of d across subjects and channels of interest, *i.e.* the ones located in the central portion of the NIRS montage that were most involved in IPS processing.

Identification of the channels of interest. We wanted to assess the characteristics of the negative BOLD responses to IPS by using the information about the hemoglobin concentration obtained by NIRS recordings. To this end, for each subject we took into account the NIRS channels with an underlying negative BOLD response with peak amplitude ≥ 1 (normalized units), whose projection was over or in proximity to the NBR regions. The number of selected channels varied from subject to subject, due to the extension of the negative BOLD responses and to the position of the NIRS optodes that varied from subject to subject.

fMRI–NIRS visual inspection. We first visually inspected the BOLD and hemoglobin signals relative to the NBR channels and excluded channels with a NIRS signal affected by high-frequency noise. A comparison between negative BOLD responses and negative/positive signs of HbO

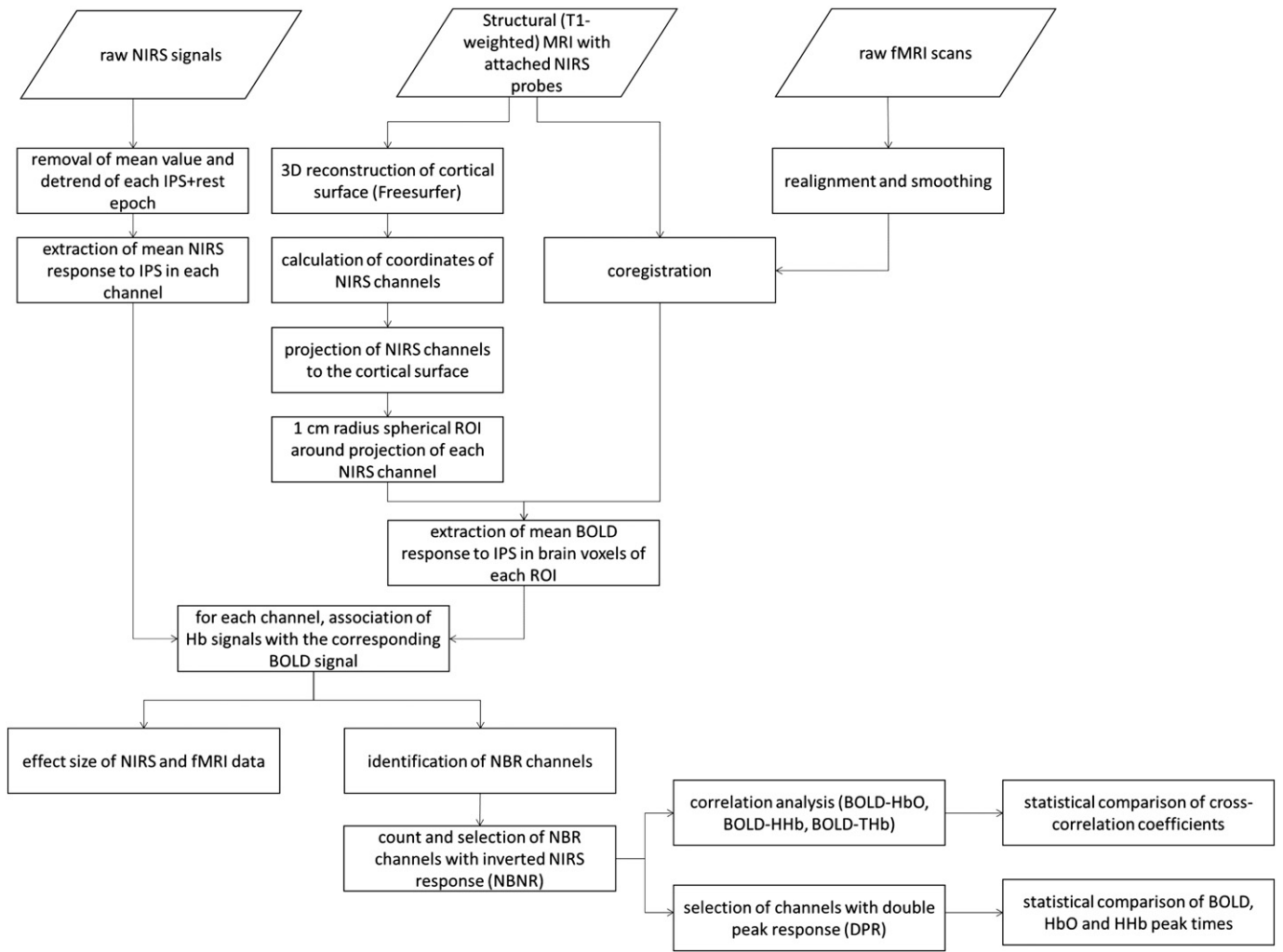


Fig. 1. Scheme of fMRI-NIRS comparison. Outline of the fMRI-NIRS comparison in each subject.

and HHb responses was performed and the number of NIRS channels located over the NBR areas showing an inverted NIRS response was counted in the single subjects.

fMRI-NIRS temporal analysis. To exclude possible confounding contributions, among the NBR channels we selected the ones having an inverted hemodynamic response in both fMRI and NIRS, clearly negative in BOLD and HbO, positive in HHb. The channels satisfying this requirement will be dubbed negative BOLD and NIRS response (NBNR) channels. The NBNR channels represented the majority of channels underlying NBRs and included the channels that were significant, as emerged from the NIRS GLM analysis. The number of NBNR channels varied from subject to subject and ranged from 1 to 5. In addition to the HbO and HHb time courses, we considered their sum as an indicator of total hemoglobin (THb).

For each NBNR channel, we calculated the correlation coefficient between BOLD and Hb time courses. For this purpose, the BOLD response was linearly upsampled to match the NIRS one. In subjects with more than one channel, a Kruskal-Wallis test was used to look for significant differences between BOLD-HbO, BOLD-HHb and BOLD-THb correlation coefficients.

The temporal relationship between BOLD and Hb signals was further investigated for a subset of NBNR channels, showing a sustained response to IPS that was characterized by a double peak pattern in both BOLD, HbO and HHb. In such channels, the beginning and ending instants of the sustained response were clearly separated and identifiable.

An example of double peak response (DPR) can be seen in Fig. 2. Although most of the NBRs showed a double peak, many Hb signals did not clearly show this pattern. For this reason, the DPR channels were selected from four out of eight subjects and the THb responses were excluded from the analysis. The times of occurrence of each peak were used to assess any time delays between BOLD, HbO and HHb peaks.

After downsampling of the NIRS responses to match the BOLD signal, the first and second peak latencies were calculated using an automatic algorithm in Matlab environment and then verified by visual inspection. The algorithm looked at the first derivative of the time series and marked as peaks the points of biggest change in derivative, e.g. from positive to negative. In each subject, the BOLD and Hb peak times were compared using a Kruskal-Wallis test. If significant differences emerged between the three species ($p < 0.01$), a pairwise comparison was performed.

Results

General Linear Model activation analysis

GLM fMRI group analysis

The results of the GLM group fixed-effect analysis on fMRI data are shown in Fig. 3 (Family Wise Error (FWE) corrected, $p < 10^{-5}$). The significant regions detected using positive and negative contrasts

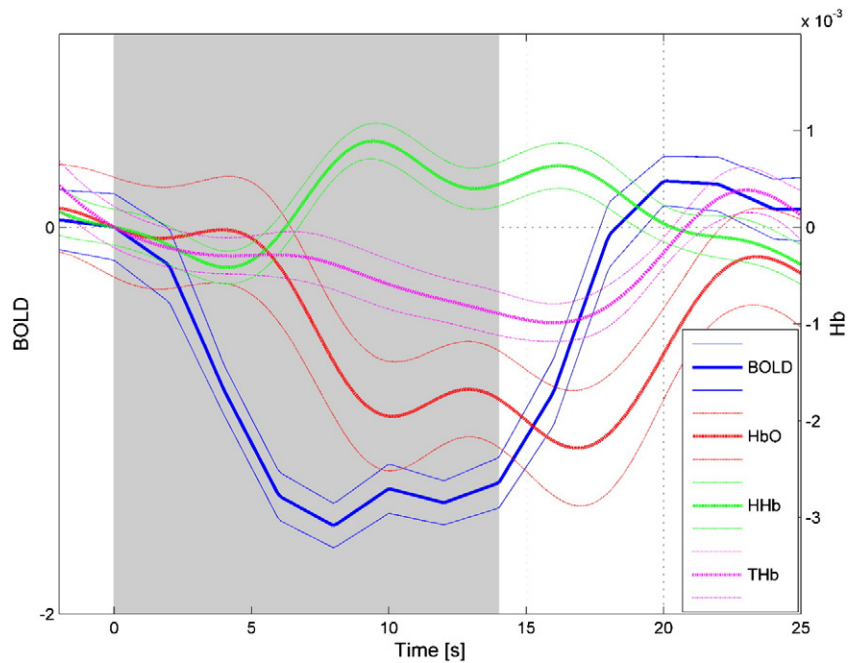


Fig. 2. BOLD-NIRS response to IPS. Plot of BOLD (blue) and hemoglobin responses (HbO red, HHb green, THb pink) to IPS in one channel (channel 3–4) of Subj1 (mean \pm SE across repetitions). The gray area corresponds to the IPS interval.

(IPS > rest, IPS < rest) are shown in red and blue respectively and discussed below.

An extended activation was elicited by photic stimulation in the primary visual cortex of both hemispheres. As expected, the area of the PBR included the calcarine cortex, the lingual gyrus and the cuneus. In addition to this expected activation, two significant NBRs were detected in two symmetrical areas belonging to the extra-striate visual cortex. The two regions were mainly located in the lateral occipital cortex of each hemisphere.

The BOLD temporal trends were extracted from the three ROIs previously identified and averaged across the eight subjects. The plot is shown in Fig. 4, relative to the three ROIs. The two symmetric regions with NBR showed a very similar temporal trend. The amplitudes of

NBRs and PBR peaks (maximum absolute values of the curves) were not significantly different. Both the PBR onset and 90% threshold times (when the curves overcome the 5% and 90% of the peak amplitude respectively) anticipated the NBRs ones, but significance was not achieved. The falling edges (the instants after the end of the IPS block when the curves decrease below 50% of the peak) of the peak were comparable too, although the NBRs showed a faster return to baseline. Results are summarized in Table 1.

GLM analysis of NIRS data

The results of GLM analysis performed on the single-subject NIRS data are displayed in Fig. 5. The results were in agreement across all eight subjects, since at least one channel in every subject showed a

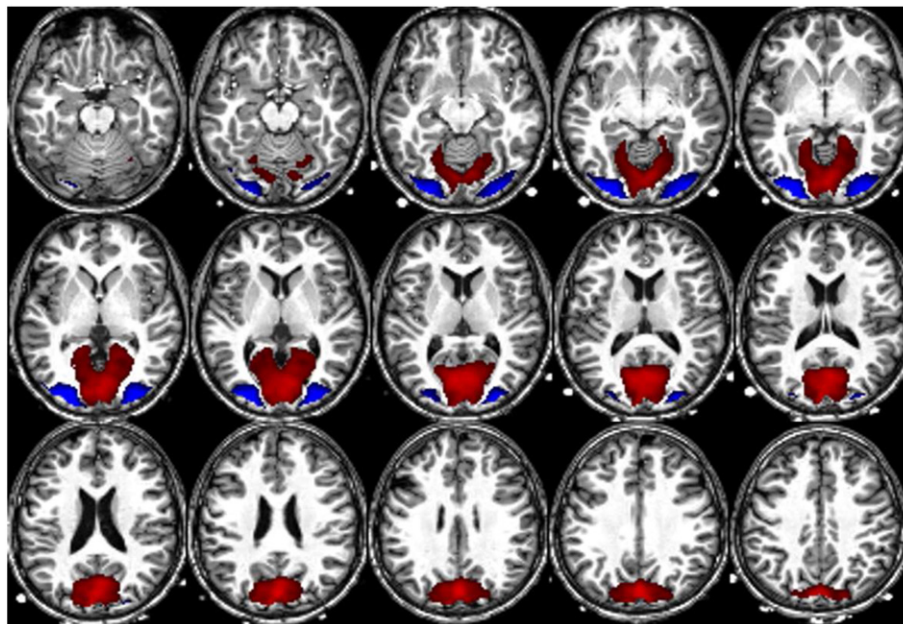


Fig. 3. fMRI GLM results. Results of the fixed-effect GLM analysis on the eight subjects. Regions with significant BOLD response to IPS (FWE corrected, $p < 10^{-5}$) projected on 15 axial slices of a representative subject in MNI space. ROIs with positive and negative response are shown in red and blue, respectively.

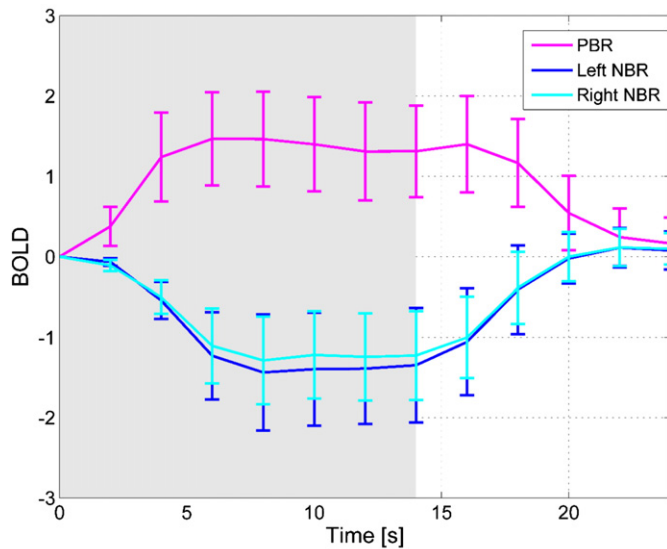


Fig. 4. Group BOLD response to IPS. BOLD responses to IPS blocks in the significant ROIs, averaged over the eight subjects (\pm standard deviation across subjects). The BOLD responses are in normalized units: they were extracted with the Marsbar toolbox of SPM8 after “Global normalization” using the default option “session-specific grand mean scaling”, which sets the mean global activity of the session to 100. Further information on grand mean scaling can be found in Friston et al. (2011). The gray background represents the stimulation period. The pink curve is relative to the PBR region, the dark and light blue curves are the left and right NBR regions, respectively.

negative NIRS response to IPS in proximity to an NBR area. Negative NIRS response is defined as a response that is inverted as compared to the canonical one. In six subjects out of eight, the two-sided t-test resulted in significant t values, positive in HHb and negative in HbO ($p < 0.05$ for at least one channel).

The negative NIRS response was characterized by an HbO decrease coupled with an HHb increase; as shown in the example in Fig. 2, such pattern persisted over the entire IPS block, until the depletion of response in the following rest period. Despite the absence of an exact symmetry of the t-statistics across the hemispheres, in six out of eight subjects the inverted response was bilateral. In the two subjects with a unilateral negative NIRS response, the overall t-test significance was very low due to signal artifacts, which were reflected in lower values of effect size as compared to the rest of the group. In each NIRS channel characterized by a negative response, the HbO response amplitude was definitely higher than the HHb one (Fig. 2). On average, the peak of HbO response was more than twice than the HHb one (2.56 ± 0.76 among subjects), thereby indicating a decrease in THb concentration.

In five subjects, one to two NIRS channels located in the primary visual cortex showed a canonical response to IPS. Nonetheless, none of them was confirmed to be significant by the t-statistics ($p < 0.05$). This result was somehow expected as the PBR to IPS involves an extended area in the medial surface of the two hemispheres and is less reachable by NIRS that can involve only the superficial cortex, with a penetration depth of about 1 cm.

Fig. 6 shows as an example the positions of NIRS channels on a subject (Subj3). The NIRS channels are projected on the reconstructed

Table 1
Time and amplitude parameters of the PBR and NBRs curves (mean value \pm standard

	Peak amplitude [n.u.]	Peak time [s]	Onset time [s]	90% peak time [s]	Falling edge [s]
PBR	1.64 ± 0.68	8.69 ± 1.77	0.59 ± 0.31	6.15 ± 1.69	4.04 ± 3.52
Left NBR	-1.58 ± 0.72	9.19 ± 1.69	0.99 ± 0.52	6.72 ± 1.54	3.33 ± 2.61
Right NBR	-1.45 ± 0.59	9.44 ± 1.24	1.06 ± 0.53	7.02 ± 1.47	3.18 ± 2.21

pial surface in native space where the fMRI significant ROIs of the subject are represented (FDR corrected, $p < 0.001$). In this subject, the most significant NIRS channels, 3–4 and 4–8, were exactly located over the NBR fMRI regions of both hemispheres. These channels, together with channel 1–4, were significant ($p < 0.05$), with very high modules of the t-statistics for both Hb species (t value ranging from 5 to 10). The HbO and HHb responses of these channels are plotted in Fig. 7. In all of them, the HbO response amplitude was greater than the HHb one, with a peak ratio of 2.29 ± 0.27 and an area ratio of 2.40 ± 0.29 . As shown by the plots, the 3–4 and 4–8 channel responses were characterized by an initial rise to the peak, followed by a sustained response with a slight descending slope that precedes the drop to baseline. In this subject, the majority of NIRS channels showed an inverted hemodynamic, although only three of them reached statistical significance.

fMRI–NIRS signal comparison

Effect size of NIRS and fMRI data

For each channel, the values of effect size d of fMRI and NIRS data are summarized in Table 2 (median value across subjects). In channels 1–4 and 4–7, both located in brain regions involved in IPS processing, the effect size of BOLD signal was significantly higher compared to each of the hemoglobin species ($p < 0.05$ in the pairwise comparisons). The median values of d across subjects and channels of interest were similar for the two hemoglobin species (0.25 for HbO, 0.31 for HHb) but lower compared to BOLD (1.41). The latter result indicates a higher IPS-related SNR in fMRI data with respect to NIRS data.

fMRI–NIRS visual inspection

The quantitative comparison between the BOLD and the NIRS responses is limited by the fact that the two modalities were recorded in different sessions, however some relevant information emerged.

The fMRI–NIRS comparison at the single channel level generally showed agreement between BOLD and Hb information. The great majority of NIRS channels corresponding to NBRs were characterized by negative HbO and positive HHb responses, as explained in detail below. In the eight subjects, there were 39 NBR channels, i.e. the NIRS channels located over the NBR regions whose underlying NBR reached a peak amplitude ≥ 1 (top row of Table 3). Among the NBR channels, 30 channels had a negative NIRS response (NBNR channels), as shown in the second row of Table 3. The median values of effect size across NBNR channels and across subjects were still higher in BOLD (2.55) compared to HbO (0.4) and HHb (0.45). Nonetheless, the hemoglobin species showed higher effect sizes in the NBNR channels compared to the rest of occipital channels. The non-NBNR occipital channels showed values of 0.87, 0.22 and 0.27 for BOLD, HbO and HHb signals, respectively.

In four subjects, a negative NIRS response corresponded to every NBR, whereas in two NBR channels of Subj7 and one of Subj8 the NIRS responses had a canonical hemodynamic pattern, probably due to the proximity of a PBR area. Three subjects (Subj2, Subj5 and Subj7) showed a biphasic hemodynamic pattern that, in some channels, made it difficult to determine the positive/negative sign of response. The biphasic response was characterized by an HbO increase over the baseline occurring before the HbO decrease that was usually observed. An example of HbO and HHb biphasic trend, relative to two channels of Subj2, is shown in Fig. 8: while in the first channel the NIRS response is clearly negative, in the second one the HbO oscillation shows a controversial pattern. Looking at the mean values of effect size across the eight central channels, it emerged that the d values of Hb signals in Subj5 and Subj7 were below 0.2 and were the lowest in the group.

fMRI–NIRS temporal analysis

The results of the correlation analysis performed on the NBNR channels of each subject are shown in the diagram in Fig. 9, while the median values of correlation coefficient across the NBNR channels of

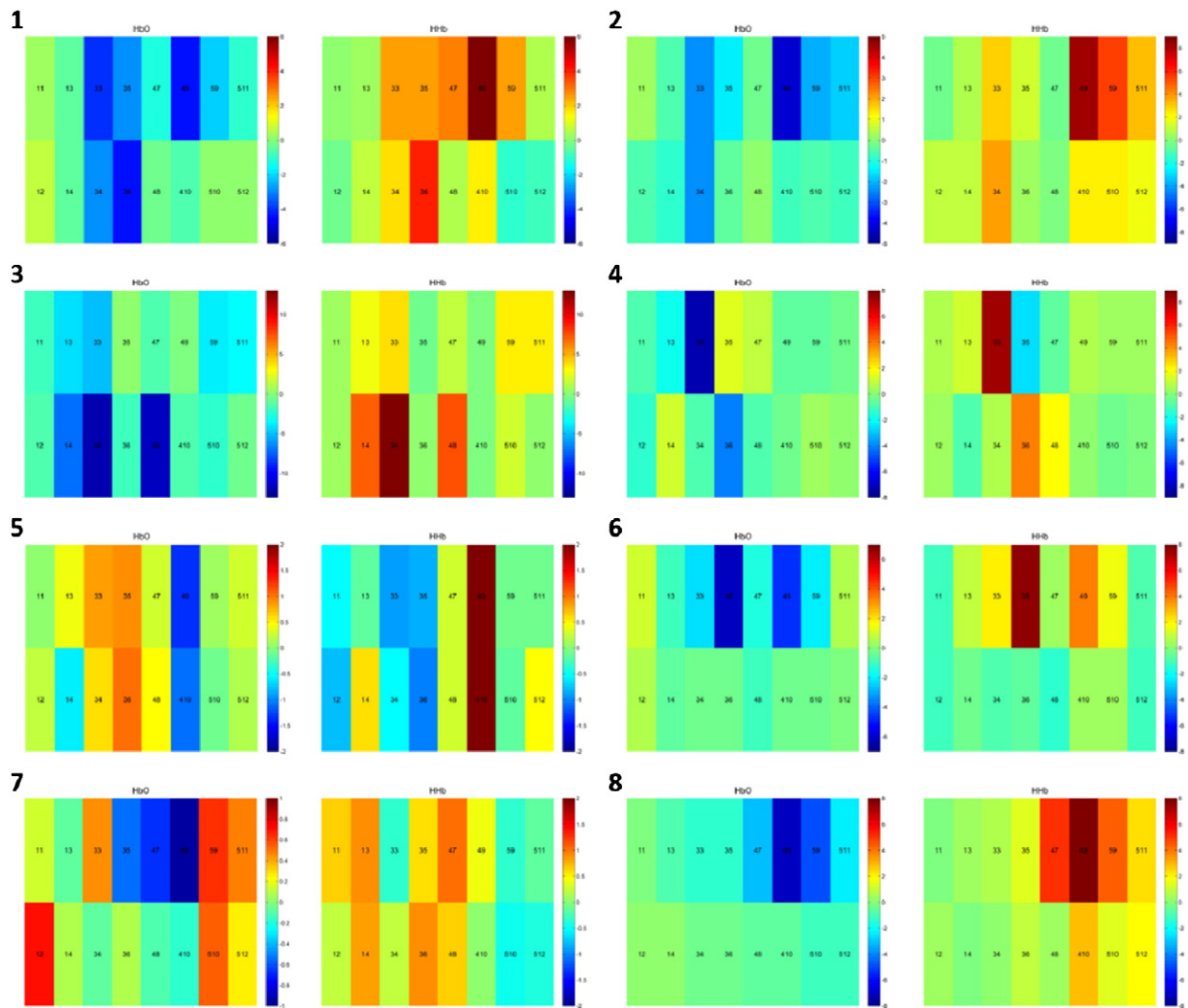


Fig. 5. NIRS GLM results. Results of GLM analysis performed on the NIRS data of the single subjects. Each rectangle is relative to one channel and shows the t-statistics value resulting from the two-sided t-test (HbO on the left, HHb on the right).

each subject are listed in Table 4. In four out of eight subjects, BOLD was more correlated to HHb, although no significant differences between the Hb species emerged from the Kruskal–Wallis test.

The DPR was detected in Subj1, Subj3, Subj6 and Subj8, in 5, 2, 3 and 2 channels respectively. The results of the time-lag analysis performed on DPR channels, which compared the times of occurrence of BOLD peaks with respect to HbO and HHb ones, are shown in Fig. 10. The peak times (median value across the DPR channels) of each subject are listed in Table 4. The BOLD peaks usually preceded the HbO and HHb ones, with the exception of Subj6, who showed BOLD and HbO responses that reached the first peak simultaneously (Table 5). The Kruskal–Wallis test, performed on each subject separately, revealed significant differences among the three species in the second peak times of Subj1 ($p < 0.01$); the subsequent pairwise comparison showed significant differences between BOLD and both HbO and HHb responses.

Discussion

In this paper, two different neuroimaging techniques, fMRI and NIRS, were employed to investigate the physiological hemodynamic response to IPS in a group of healthy subjects. The NIRS technique was introduced to extend the fMRI study, which revealed the presence of two symmetric regions in extra-striate visual cortex having a significant negative BOLD response, *i.e.* inverted with respect to the canonical HRF. NIRS offers the advantage to separate the dynamics of HbO and HHb, thus providing a better insight into the physiological mechanisms involved in the genesis of the BOLD response. On the other hand, NIRS probing capabilities are limited to the cortex surface. The integration of the two modalities

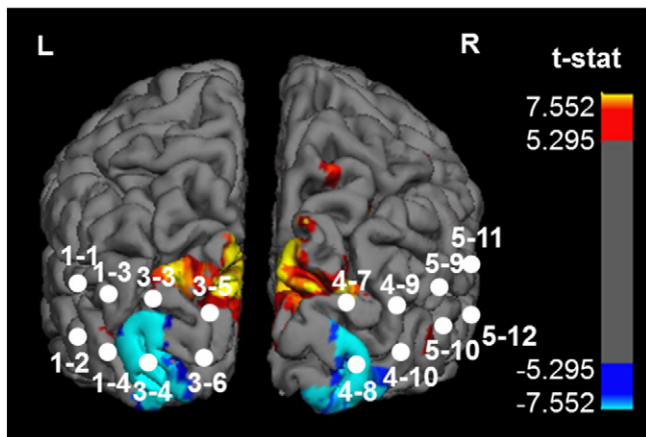


Fig. 6. NIRS–fMRI coregistration. Coregistration of NIRS channels and fMRI data in Subj3. The significant ROIs of the single-subject GLM analysis in native space (FDR corrected, $p < 0.001$) are represented on the reconstructed pial surface of the subject (PBR in red, NBRs in blue). The NIRS channels are projected on the same surface.

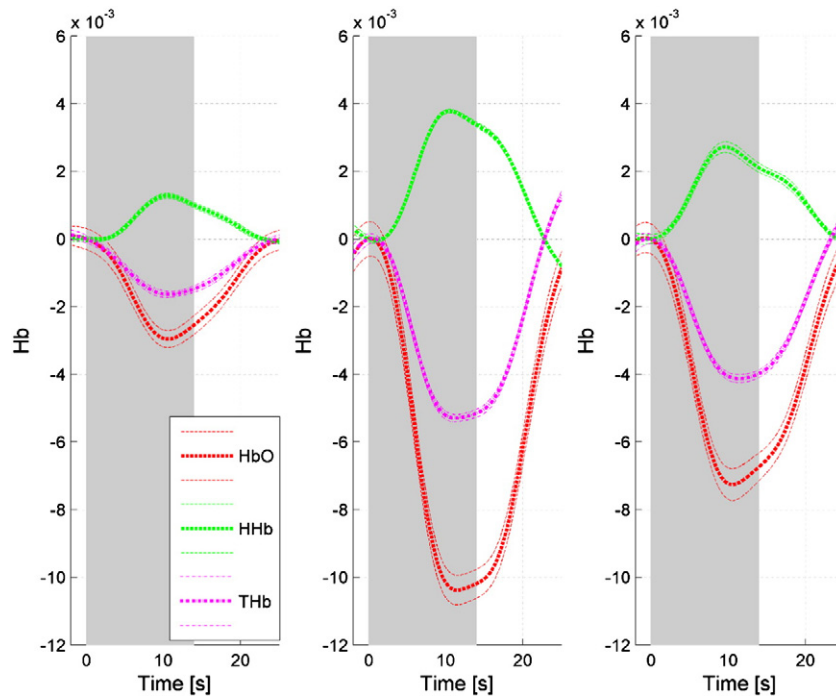


Fig. 7. Negative NIRS responses to IPS. HbO (red dashed), HHb (green dashed and dotted) and THb responses to IPS (mean \pm SE across repetitions) in the three channels of Subj3 (1–4, 3–3 and 3–4) with significant negative NIRS response to IPS ($p < 0.05$).

allows for a more complete analysis of the hemodynamic physiological response to IPS. In our study, NIRS has confirmed the presence of an inverted hemodynamic response and moreover has characterized the negative BOLD phenomenon in terms of oxygenation changes.

Negative BOLD findings

The emergence of negative BOLD responses to visual stimulations has been already described in literature; nonetheless, our study is the first reporting such extended and symmetric NBRs in the presence of simple IPS. Previous studies on negative BOLD responses used more complex visual stimulation, such as flickering Gabors, checkers or bars (Tootell et al., 1998; Smith et al., 2000; Shmuel et al., 2002; Bressler et al., 2007). In many of them, a BOLD increase with respect to rest emerged in the cortical regions involved in the stimulus processing, in combination with a BOLD decrease in the surrounding visual regions. However, by using visual stimuli restricted to one hemifield, it was demonstrated that the NBR could also be spatially remote from the PBR (Tootell et al., 1998; Smith et al., 2004). In our study, the two NBRs were more lateral and superficial than the significant PBR in the primary visual cortex, next to it but segregated. The high significance of the NBRs across subjects was demonstrated by their relevant amplitude, which was comparable to the PBR one. The temporal properties of the two symmetric NBRs were the same, while slight differences were detected with respect to PBR, consisting of delayed onset time and peak time, earlier falling edge and faster return to baseline. On the other hand, it is worth remembering that positive and negative re-sponses were located in different areas, and small differences in hemo-dynamic responses cannot be excluded. The delay of NBRs *versus* PBR

had already been observed in previous works (Shmuel et al., 2006; Goense et al., 2012). These temporal differences excited further interest towards the negative BOLD phenomenon.

On the origin of NBR

The mechanism accounting for negative BOLD responses has never been completely explained. According to the “vascular stealing” interpretation, the oxygenated blood available at one time is limited, therefore it is supplied proportionally to the request. As a consequence, during a task, the oxygen that serves the activated areas would be subtracted from the uninvolved neighboring areas. The “blood stealing” was considered as a possible explanation for NBRs in Shmuel et al.(2002), and could be also compatible with a delayed NBR. On the other hand, the same authors suggested that the NBRs could be triggered by a reduction in neuronal activity. The main evidence for that was the decrease in both measured cerebral blood flow (CBF) and estimated oxygen consumption (CMRO₂) in the regions exhibiting NBRs.

In later works, the neuronal inhibition hypothesis has been largely favored over the vascular one (Wade, 2002; Smith et al., 2004; Bressler et al., 2007; Mullinger et al., 2014), although the scope of the reduced neuronal activity is still debated. The most supported theory is based on attentional modulation processes, which would improve the accuracy of stimulus processing by increasing the neuronal activity in the involved sites while suppressing activation in the uninvolved locations (Müller and Kleinschmidt, 2004; Maunsell and Cook, 2002); the NBRs would thus be considered as active contributors to the attentional process. This hypothesis is in line with the properties of NBRs,

Table 2

Effect size d of BOLD, HbO and HHb signals corresponding to each NIRS channel (median value across subjects). The position of channels is shown in Fig. 6.

	Ch. 1–1	Ch. 1–2	Ch. 1–3	Ch. 1–4	Ch. 3–3	Ch. 3–4	Ch. 3–5	Ch. 3–6	Ch. 4–7	Ch. 4–8	Ch. 4–9	Ch. 4–10	Ch. 5–9	Ch. 5–10	Ch. 5–11	Ch. 5–12
BOLD	0.17	0.33	0.38	0.99	2.76	2.47	1.59	0.91	1.26	0.33	1.55	1.13	0.40	0.44	0.06	0.10
HbO	0.10	0.21	0.20	0.12	0.62	0.16	0.51	0.24	0.26	0.10	0.71	0.10	0.43	0.17	0.25	0.16
HHb	0.11	0.19	0.18	0.19	0.67	0.18	0.52	0.26	0.30	0.21	0.87	0.32	0.69	0.19	0.31	0.23

Table 3
NIRS channels corresponding to NBRs (first row) and with an inverted NIRS response (second row).

	Subj1	Subj2	Subj3	Subj4	Subj5	Subj6	Subj7	Subj8
# NIRS channels with NBRs	5	7	4	2	2	5	9	5
# channels with inverted NIRS response	5	4	4	2	1	5	5	4

which have been shown to carry specific spatial information about the visual stimuli (Bressler et al., 2007). This study suggested that neuronal suppression, and the concomitant negative BOLD response, may play a key role in the top-down attentional system.

In our fMRI study, the fact that the NBRs are spatially segregated from the PBR makes the vascular hypothesis less likely or at least not sufficient to explain the phenomenon. Although not statistically significant, the differences in temporal trend between positive and negative curves point towards a neuronal origin of the phenomenon. Moreover, the NBRs induced by IPS exhibited a higher amplitude as compared to many visual NBRs that have been described so far (Goense et al., 2012; Huber et al., 2014). This finding could suggest a main contribution of negative responses in the processing of IPS, raising further questions on their underlying mechanisms.

Investigation of NBRs with optical imaging

Although some vascular parameters of visual NBRs have already been investigated in both macaques and humans (Shmuel et al., 2002; Goense et al., 2012; Huber et al., 2014), a full hemodynamic characterization of this phenomenon is still lacking. In the present study, the NIRS technique was introduced to 1) check whether the negative BOLD pattern corresponded to negative NIRS responses and 2) gain further insight into the NBR characteristics based on changes in HbO, HHb and THb levels. The NIRS technique measures the main constituents of BOLD signal changes, therefore it can provide valuable clues as to the negative BOLD phenomenon.

To the best of our knowledge, this is the first time that NBRs to visual stimuli are investigated with the help of an optical imaging technique. The NIRS study provided a useful contribution to NBR analysis: indeed, it confirmed the presence of a negative hemodynamic response to IPS in the lateral occipital cortex and provided new evidences of the NBR vascular properties, which are discussed hereinafter.

The canonical vascular response to a stimulus is characterized by a vasodilation and higher blood oxygenation, with increase in HbO and decrease in HHb concentrations, according to the Balloon model (Buxton et al., 1998). By contrast, during IPS, we recorded an HbO decrease and a concomitant HHb increase *versus* baseline in the extrastriate visual areas. The signal changes for HHb were smaller than those for HbO, similarly to the canonical response but with inverted course, thus resulting in a THb decrease. Since the latter proved to be an accurate measure of changes in CBV (Toronov et al., 2003), the results suggest that the negative NIRS response, which in turn corresponds to NBR, is associated to a CBV decrease (*i.e.* vasoconstriction). This finding is consistent with findings in humans described in Huber et al. (2014) but not in monkeys (Huber et al., 2014; Goense et al., 2012). In the human experiment of (Huber et al., 2014), where venous and arterial CBVs were evaluated separately, it additionally emerged that the CBV contribution to NBR was mainly related to the larger superficial arterial compartment.

Despite no CBF measures were provided in our study, based on the Hb changes we cannot exclude the CBF decrease in the NBR regions measured in Pasley et al. (2007), Goense et al. (2012) and Huber et al. (2014). In line of principle, the HHb increase and HbO decrease measured during IPS can be due either to 1) an increase in CMRO₂ with no CBF change, 2) a decrease in CBF with no CMRO₂ change, 3) an increase in CMRO₂ with a decrease in CBF, 4) an increase in CBF with a bigger increase in CMRO₂ or 5) a decrease in CMRO₂ with a bigger decrease in CBF. However, our NIRS results additionally revealed that the HbO decrease was higher than the HHb increase: this new evidence is in favor of the last two hypotheses. In particular, hypothesis n.5, according to which NBR are caused by decreases in both CBF and CMRO₂, is consistent with the idea that NBR reflects neuronal deactivation and is currently considered the most likely physiological cause of NBR (Mullinger et al., 2014).

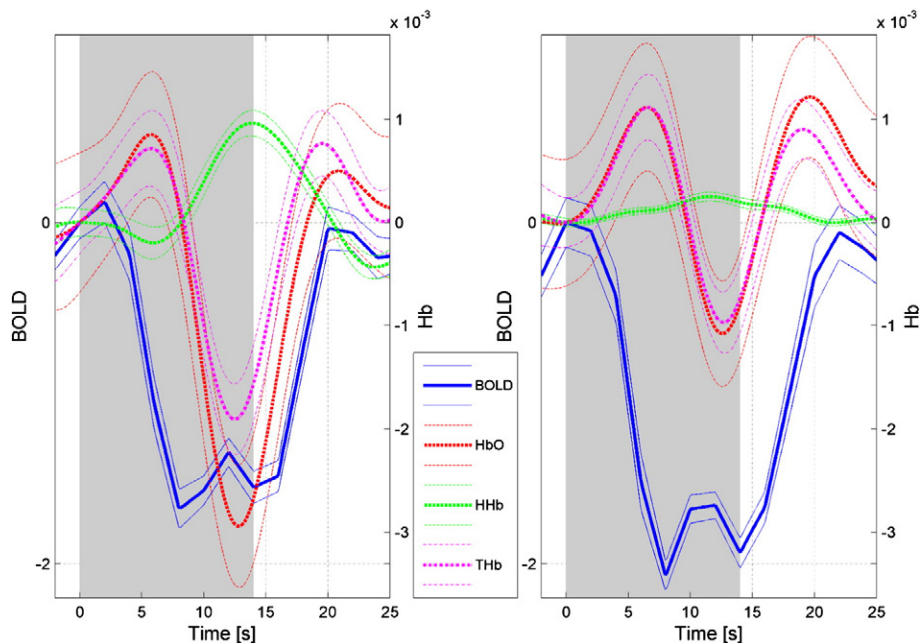


Fig. 8. Biphasic NIRS responses to IPS. Plot of BOLD (blue) and hemoglobin responses (HbO red, HHb green, THb pink) to IPS in two channels of Subj2 with biphasic pattern (channel 3–3 on the left, channel 4–10 on the right) (mean \pm SE across repetitions). The negative response is clearly visible on the left, controversial on the right.

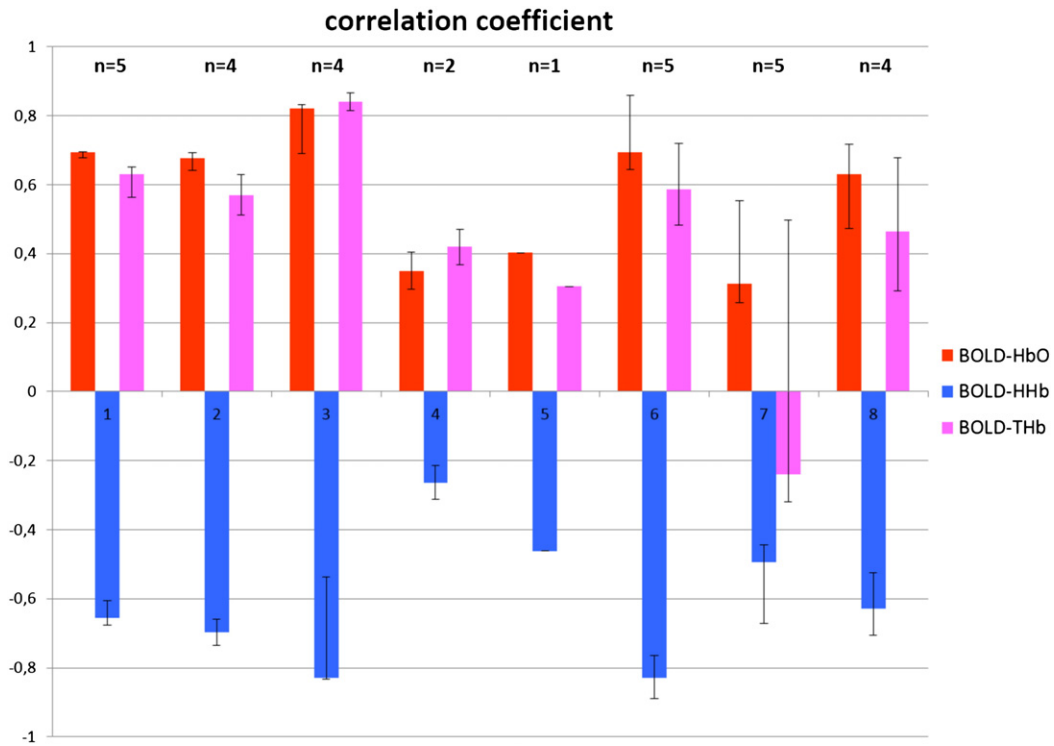


Fig. 9. Correlation analysis results. Values of correlation between BOLD and Hb species for each subject (median across the NBNR channels of each subject, error bars 25 and 75 percentiles). BOLD-HbO: red bars; BOLD-HHb: blue bars; BOLD-THb: pink bars. n = number of NIRS channels used for each subject.

Literature on inverted NIRS response in the visual cortex

Among the many NIRS studies on human visual cortical functions (e.g. Kato et al., 1993; Toronov et al., 2006; Jaszewski et al., 2003; Seiyama et al., 2003), only a few detected the presence of a negative NIRS responses to visual stimuli (Gratton et al., 2001; Watanabe et al., 2012). In a study on healthy subjects, Gratton and colleagues stimulated with a vertical grid pattern reversal and found a negative NIRS response in approximately the same region as our study. However, this finding was not discussed and no information about HbO and HHb contributions were available. Watanabe et al. (2012) used NIRS to examine the effect of visual stimuli on cortical processing in 6-months old infants. While stimulating with high luminance unpatterned screens (without reversal), they found in the occipital cortex a transient increase followed by a salient decrease in HbO response and an opposite trend for HHb, which was interpreted as an initial activation followed by deactivation. The aim of such work was to extend findings from previous studies on sleeping children showing deactivations, as it showed that a negative response to visual stimulation could also occur in children in the awake state. However, the authors considered the biphasic response as an ability of infants to switch from activation to deactivation whenever a structureless visual stimulation was presented instead of a meaningful one. Our study provided new evidence as it showed that adults, too, are characterized by an inverted hemodynamic response to intermittent unpatterned visual stimulation. Similarly to children in (Watanabe et al. 2012), three of our subjects showed a biphasic NIRS

response, consisting of an initial canonical pattern (increase in HbO and decrease in HHb, with the latter usually lower than the former) followed by an inversion. This pattern may be due to noise in the NIRS recordings, a hypothesis which is in line with the low mean values for the effect size of the NIRS signals in these subjects. Alternatively, it could indicate a shift from a state of activation to a state of suppression, as suggested in Watanabe et al. (2012). Such transient change could be due to a redirection of blood supply to neighboring active areas of the cortex.

Differently from the just mentioned NIRS studies, which focused on inverted NIRS responses in the visual cortex, in our study hemodynamics was investigated by means of both fMRI and NIRS and the temporal properties of BOLD responses were compared to Hb ones. The main limitation of our study is that fMRI and NIRS acquisitions were performed in separate sessions, due to the impossibility to use the NIRS device within the MR scanner. Nevertheless, since the response of healthy subjects to IPS blocks has very limited intra-subject variability, a comparison across non-simultaneous modalities is feasible. Furthermore, the structural MRI performed in association to both NIRS and fMRI acquisition allowed for the spatial coregistration between the two functional modalities.

Correlation between NBRs and hemoglobin species

In the literature, simultaneous NIRS-fMRI studies investigated whether BOLD was more correlated (in space and time) to one of the chromophores, but findings are rather inhomogeneous. A number of studies showed BOLD signal to be more correlated in time to HHb than to HbO and THb signals (Siegel et al., 2003; Huppert et al., 2006). This finding is supported by theoretical knowledge, according to which fMRI BOLD contrast arises from HHb paramagnetic properties. On the other hand, controversial findings emerged from other studies, such as Hess et al. (2000) and Strangman et al. (2002), where the THb was found to be more correlated to BOLD than the HHb.

So far, the great majority of simultaneous fMRI-NIRS studies investigated motor and somato-sensory cortex activations, while only a few

Table 4
Median of correlation coefficients between BOLD and Hb species across the negative BOLD and NIRS response (NBNR) channels of each subject.

	Subj1	Subj2	Subj3	Subj4	Subj5	Subj6	Subj7	Subj8
BOLD-HbO	0.70	0.68	0.82	0.35	0.40	0.69	0.31	0.63
BOLD-HHb	-0.66	-0.70	-0.83	-0.26	-0.46	-0.83	-0.49	-0.63
BOLD-THb	0.63	0.57	0.84	0.42	0.31	0.59	-0.24	0.47

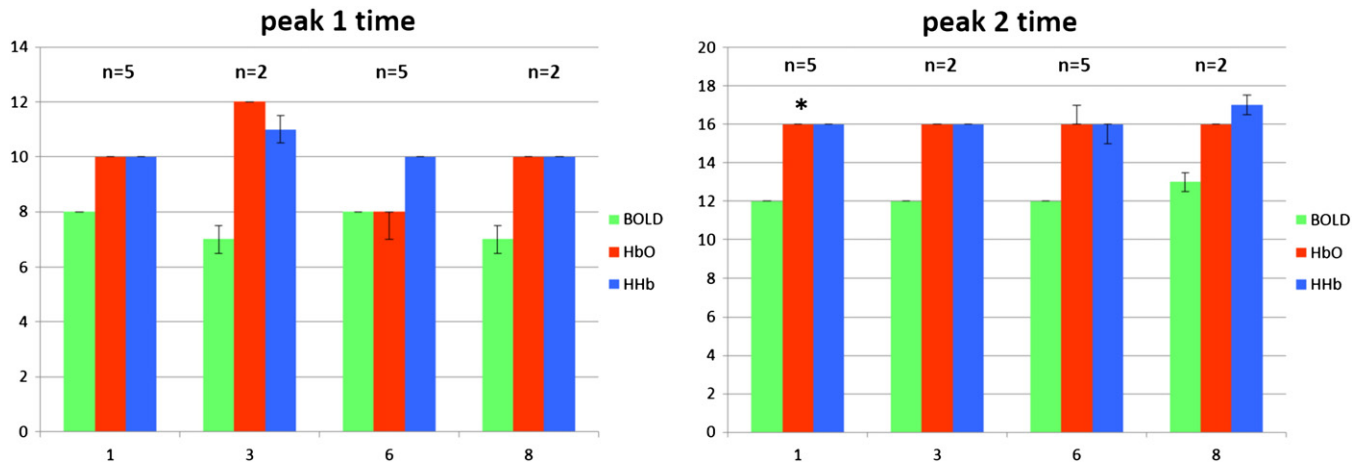


Fig. 10. Time-lag analysis results. Comparison between peak times of BOLD, HbO and HHb response to IPS in the four subjects with DPR (median value across DPR channels, error bars 25 and 75 percentiles). * = significant differences ($p < 0.01$). n = number of NIRS channels used for each subject.

focused on the visual cortex (Schroeter et al., 2006; Toronov et al., 2006). Since the mechanism of cerebral vascular response has been shown to have regional differences (Gotoh et al., 2001), the coupling dynamics in different brain areas may be different (Lu et al., 2004); therefore, our study should be better compared to other visual NIRS-fMRI studies. In the early visual cortex, Schroeter et al. (2006) found the strongest temporal correlation between BOLD and HHb, whereas Toronov et al. (2006) detected a better spatial and temporal link between BOLD and both HbO and THb than the HHb. Furthermore, these calculations were performed on positive BOLD responses, differently from our study.

We found a consistent spatial correlation between negative BOLD responses and the corresponding Hb signals, since in all our subjects the channels with inverted NIRS response were located over or in proximity to NBR regions. The opposite was not always verified, since few NIRS channels that were over the NBRs showed either a biphasic or a positive NIRS response. The possible reasons for this discrepancy are to be found in the lower CNR of HbO and HHb signals compared to BOLD, adjacency of positive and negative BOLD responses or imprecisions in the spatial coregistration of the NIRS and fMRI results. The gap of CNR between NIRS and fMRI data that emerged in our study may be related to the sensitivity of the NIRS technique to a number of subjective factors, such as color and quantity of hair, color of the skin and scalp-brain distance, which do not affect the fMRI data quality.

Despite the good spatial agreement between NIRS and fMRI data, heterogeneous values of correlation coefficients between HbO-BOLD, HHb-BOLD and THb-BOLD signal pairs were detected. We could explain such variability by looking at the temporal coupling between BOLD and each Hb species, which was rather variable from subject to subject.

In particular, half of the subjects were characterized by a clear double-peak response to IPS blocks in HbO, HHb and BOLD. In the subjects showing DPR, the BOLD peaks usually preceded the HbO and HHb ones. In this group, the Hb delay was caused by either an initial

dip in HHb response that was not present in NBR or by a minor slope of Hb response *versus* BOLD response at the onset of IPS. In the other four subjects, the temporal coupling between BOLD and Hb responses was less homogeneous. The BOLD-Hb delays contributed to reducing the correlation of BOLD and Hb species.

The low temporal correlation between BOLD and Hb responses, particularly visible in the DPR channels, is an unusual finding that still lacks a definite explanation. First, it is important to keep in mind that the acquisitions were made in different sessions, thus it is difficult to provide a precise interpretation of temporal relations. Such inhomogeneity could be caused by systematic measurement errors, differences in the temporal resolution of NIRS and fMRI signals or by NIRS sensitivity to superficial hemodynamic fluctuations. Another factor that deserves attention concerns the definition of the NIRS sensitivity region, from which the BOLD response is extracted. In our study, we considered the brain voxels within a sphere centered in the projection of the NIRS channel to the cortical surface, similarly to Okamoto et al. (2004) and Cui et al. (2011). Although this method has been found to be reliable, a comparison among different path shapes and approaches (for example, considering only correlated voxels) could be an interesting focus of future research.

The different sensitivity of NIRS and fMRI measures could also contribute to the time delay between NIRS and fMRI signals. If we assume that NIRS is more sensitive to the microvasculature and that BOLD signal represents all spatial scales of venous vessels (Schroeter et al., 2006), we could hypothesize that a decrease in post-capillary venous washout occurred from the onset of stimulation, causing the immediate decrease in BOLD signal, while in the capillary compartment the hemodynamic inversion (decrease in HbO and increase in HHb) begun with a delay of few seconds.

We should also consider that pial veins could also be partly responsible for the differences between NIRS and fMRI responses. The NIRS signal is integrated through the different superficial layers of the head, with the risk of being contaminated by the pial veins intersecting the photon path (Gagnon et al., 2012). By contrast, such risk should be negligible in fMRI, where the higher spatial resolution allows separating the cortical from the pial contribution. As a final alternative, the temporal delay between NIRS and fMRI response could be peculiar to negative BOLD responses, since it was not detected in other NIRS-fMRI studies that focused on positive BOLD responses. These hypotheses, especially the latter, need to be verified in further studies.

Future perspectives

Several studies showed that a multimodal approach is essential for developing a comprehensive view of the negative BOLD phenomenon.

Table 5
Median of peak times across the double-peak response (DPR) channels of each subject.

	Subj1	Subj3	Subj6	Subj8
<i>First peak time [s]</i>				
BOLD	8	7	8	7
HbO	10	12	8	10
HHb	10	11	10	10
<i>Second peak time [s]</i>				
BOLD	12	12	12	13
HbO	16	16	16	16
HHb	16	16	16	17

Despite the fact that the NIRS technique suffers from limitations (e.g. low spatial resolution and superficial information), it provided useful information for the characterization of NBR and was confirmed to be a valuable tool complementary to fMRI. However, there are still open questions arising from the present study that should be addressed in the near future.

Our fMRI study highlighted differences in the temporal properties of positive and negative BOLD responses, which however were not investigated by NIRS due to the absence of NIRS channels significantly activated from IPS. Future NIRS–fMRI studies employing different stimulation protocols could shed light on the vascular differences between positive and negative BOLD responses. Moreover, the use of fMRI BOLD contrast with higher resolution could allow for the discrimination of venous from arterial contributions, thereby making the integration of NIRS and fMRI information more accurate.

Finally, the future combination of NIRS and fMRI with electrophysiological recordings and measures of CBF, CBV and CMRO₂ will provide a comprehensive view of the neurovascular origin of negative BOLD responses in the human brain.

Conclusions

In the present study, we investigated negative BOLD responses to visual stimulation in healthy subjects by means of an optical technique, NIRS, which can provide insight into the vascular and hemodynamic determinants of BOLD responses. The NIRS results were consistent with the fMRI ones, since they confirmed a negative hemodynamic response in correspondence of NBRs, and additionally provided new evidence for the negative BOLD phenomenon. We found NBRs to be related to an accumulation of HHb concomitant to a higher decrease in HbO, which in turn was associated to a THb decrease. The temporal coupling between BOLD and Hb signals was rather variable within the group, therefore it should be further investigated. The main novelty of our study with respect to previous studies on negative BOLD is that it investigated this phenomenon from a different perspective. The HbO and HHb changes were confirmed to be key elements in the investigation of the hemodynamic control mechanisms underlying negative BOLD responses.

Acknowledgments

Grant support was provided by Fondazione Cariplo (project #2010-0344, “Spider@Lecco”).

References

Arrigoni, F., Maggioni, E., Zucca, C., Bianchi, A.M., Reni, G., Triulzi, F.M., 2013. Symmetric negative BOLD signal in extrastriate visual cortex during intermittent photic stimulation. Abstract at 19th Annual Meeting of the Organization for Human Brain Mapping, June 16–20, 2013, Seattle, WA, USA.

Beckmann, C.F., Jenkinson, M., Smith, S.M., 2003. General multilevel linear modeling for group analysis in fMRI. *NeuroImage* 20 (2), 1052–1063.

Bressler, D., Spotswood, N., Whitney, D., 2007. Negative BOLD fMRI response in the visual cortex carries precise stimulus-specific information. *PLoS One* 2 (5), e410.

Brett, M., Anton, J., Valabregue, R., Poline, J., 2002. Region of interest analysis using the MarsBar toolbox for SPM 99. *NeuroImage* 16, S497.

Buxton, R.B., Wong, E.C., Frank, L.R., 1998. Dynamics of blood flow and oxygenation changes during brain activation: the balloon model. *Magn. Reson. Med.* 39 (6), 855–864.

Cohen, J., 1992. A power primer. *Psychol. Bull.* 112 (1), 155.

Cui, X., Bray, S., Bryant, D.M., Glover, G.H., Reiss, A.L., 2011. A quantitative comparison of NIRS and fMRI across multiple cognitive tasks. *NeuroImage* 54 (4), 2808–2821.

Dale, A.M., Fischl, B., Sereno, M.I., 1999. Cortical surface-based analysis: I. segmentation and surface reconstruction. *NeuroImage* 9 (2), 179–194.

Devor, A., Tian, P., Nishimura, N., Teng, L.C., Hillman, E.M., Narayanan, S.N., Ulbert, L., Boas, D.A., Kleinfeld, D., Dale, A.M., 2007. Suppressed neuronal activity and concurrent arteriolar vasoconstriction may explain negative blood oxygenation level-dependent signal. *J. Neurosci. Off. J. Soc. Neurosci.* 27 (16), 4452–4459.

Friston, K.J., Ashburner, J.T., Kiebel, S.J., Nichols, T.E., Penny, W.D., 2011. *Statistical Parametric Mapping: The Analysis of Functional Brain Images*. Academic Press.

Gagnon, L., Yücel, M.A., Dehaes, M., Cooper, R.J., Perdue, K.L., Selb, J., Huppert, T.J., Hoge, R.D., Boas, D.A., 2012. Quantification of the cortical contribution to the NIRS signal

over the motor cortex using concurrent NIRS–fMRI measurements. *NeuroImage* 59 (4), 3933–3940.

Goense, J., Merkle, H., Logothetis, N.K., 2012. High-resolution fMRI reveals laminar differences in neurovascular coupling between positive and negative BOLD responses. *Neuron* 76 (3), 629–639.

Gotoh, J., Kuang, T., Nakao, Y., Cohen, D.M., Melzer, P., Itoh, Y., Pak, H., Pettigrew, K., Sokoloff, L., 2001. Regional differences in mechanisms of cerebral circulatory response to neuronal activation. *Am. J. Physiol. Heart Circ. Physiol.* 49 (2), H821.

Gratton, G., Goodman-Wood, M.R., Fabiani, M., 2001. Comparison of neuronal and hemodynamic measures of the brain response to visual stimulation: an optical imaging study. *Hum. Brain Mapp.* 13 (1), 13–25.

Hamzei, F., Dettmers, C., Rzanny, R., Liepert, J., Büchel, C., Weiller, C., 2002. Reduction of excitability (“inhibition”) in the ipsilateral primary motor cortex is mirrored by fMRI signal decreases. *NeuroImage* 17 (1), 490–496.

Hess, A., Stiller, D., Kaulisch, T., Heil, P., Scheich, H., 2000. New insights into the hemodynamic blood oxygenation level-dependent response through combination of functional magnetic resonance imaging and optical recording in gerbil barrel cortex. *J. Neurosci. Off. J. Soc. Neurosci.* 20 (9), 3328–3338.

Huber, L., Goense, J., Kennerley, A.J., Ivanov, D., Krieger, S.N., Lepsien, J., Trampel, R., Turner, R., Möller, H.E., 2012. Investigation of the neurovascular coupling in positive and negative BOLD responses in human brain at 7 T. *NeuroImage* 97, 349–362.

Huppert, T., Hoge, R., Diamond, S., Franceschini, M.A., Boas, D.A., 2006. A temporal comparison of BOLD, ASL, and NIRS hemodynamic responses to motor stimuli in adult humans. *NeuroImage* 29 (2), 368–382.

Jasdzewski, G., Strangman, G., Wagner, J., Kwong, K., Poldrack, R., Boas, D., 2003. Differences in the hemodynamic response to event-related motor and visual paradigms as measured by near-infrared spectroscopy. *NeuroImage* 20 (1), 479–488.

Kastrup, A., Baudewig, J., Schnaudigel, S., Huonker, R., Becker, L., Sohns, J.M., Dechent, P., Klingner, C., Witte, O.W., 2008. Behavioral correlates of negative BOLD signal changes in the primary somatosensory cortex. *NeuroImage* 41 (4), 1364–1371.

Kato, T., Kamei, A., Takashima, S., Ozaki, T., 1993. Human visual cortical function during photic stimulation monitoring by means of near-infrared spectroscopy. *J. Cereb. Blood Flow Metab.* 13, 516–516.

Larsson, J., Heeger, D.J., 2006. Two retinotopic visual areas in human lateral occipital cortex. *J. Neurosci. Off. J. Soc. Neurosci.* 26 (51), 13128–13142.

Logothetis, N.K., Pauls, J., Augath, M., Trinath, T., Oeltermann, A., 2001. Neurophysiological investigation of the basis of the fMRI signal. *Nature* 412 (6843), 150–157.

Lu, H., Golay, X., Pekar, J.J., Van Zijl, P.C., 2004. Sustained poststimulus elevation in cerebral oxygen utilization after vascular recovery. *J. Cereb. Blood Flow Metab.* 24 (7), 764–770.

Maggioni, E., Molteni, E., Arrigoni, F., Zucca, C., Reni, G., Triulzi, F., Bianchi, A., 2013. Coupling of fMRI and NIRS measurements in the study of negative BOLD response to intermittent photic stimulation. *Engineering in Medicine and Biology Society (EMBC), 2013 35th Annual International IEEE EMBS Conference of the IEEE*, pp. 1378–1381. <http://dx.doi.org/10.1109/EMBC.2013.6609766>.

Maunsell, J.H., Cook, E.P., 2002. The role of attention in visual processing. *Philos. Trans. R. Soc. Lond. Ser. B Biol. Sci.* 357 (1424), 1063–1072.

Moosmann, M., Ritter, P., Krastel, I., Brink, A., Thees, S., Blankenburg, F., Taskin, B., Obrig, H., Villringer, A., 2003. Correlates of alpha rhythm in functional magnetic resonance imaging and near infrared spectroscopy. *NeuroImage* 20 (1), 145–158.

Müller, N.G., Kleinschmidt, A., 2004. The attentional ‘spotlight’s penumbra: center-surround modulation in striate cortex. *Neuroreport* 15 (6), 977–980.

Mullinger, K., Mayhew, S., Bagshaw, A., Bowtell, R., Francis, S., 2014. Evidence that the negative BOLD response is neuronal in origin: a simultaneous EEG–BOLD–CBF study in humans. *NeuroImage* 94, 263–274.

Ogawa, S., Lee, T.M., Kay, A.R., Tank, D.W., 1990. Brain magnetic resonance imaging with contrast dependent on blood oxygenation. *Proc. Natl. Acad. Sci. U. S. A.* 87 (24), 9868–9872.

Okamoto, M., Dan, H., Shimizu, K., Takeo, K., Amita, T., Oda, I., Konishi, I., Sakamoto, K., Isobe, S., Suzuki, T., 2004. Multimodal assessment of cortical activation during apple peeling by NIRS and fMRI. *NeuroImage* 21 (4), 1275–1288.

Pasley, B.N., Inglis, B.A., Freeman, R.D., 2007. Analysis of oxygen metabolism implies a neural origin for the negative BOLD response in human visual cortex. *NeuroImage* 36 (2), 269–276.

Plichta, M.M., Heinzel, S., Ehlis, A., Pauli, P., Fallgatter, A.J., 2007. Model-based analysis of rapid event-related functional near-infrared spectroscopy (NIRS) data: A parametric validation study. *NeuroImage* 35 (2), 625–634.

Schäfer, K., Blankenburg, F., Kupers, R., Grüner, J.M., Law, I., Lauritzen, M., Larsson, H.B., 2012. Negative BOLD signal changes in ipsilateral primary somatosensory cortex are associated with perfusion decreases and behavioral evidence for functional inhibition. *NeuroImage* 59 (4), 3119–3127.

Schroeter, M.L., Kupka, T., Mildner, T., Uludağ, K., Von Cramon, D.Y., 2006. Investigating the post-stimulus undershoot of the BOLD signal—a simultaneous fMRI and fNIRS study. *NeuroImage* 30 (2), 349–358.

Seiyama, A., Seki, J., Tanabe, H.C., Ooi, Y., Satomura, Y., Fujisaki, H., Yanagida, T., 2003. Regulation of oxygen transport during brain activation: stimulus-induced hemodynamic responses in human and animal cortices. *Dyn. Med.* 2 (1), 6.

Shmuel, A., Yacoub, E., Pfeuffer, J., Van de Moortele, P., Adriany, G., Hu, X., Ugurbil, K., 2002. Sustained negative BOLD, blood flow and oxygen consumption response and its coupling to the positive response in the human brain. *Neuron* 36 (6), 1195–1210.

Shmuel, A., Augath, M., Oeltermann, A., Logothetis, N.K., 2006. Negative functional MRI response correlates with decreases in neuronal activity in monkey visual area V1. *Nat. Neurosci.* 9 (4), 569–577.

Siegel, A.M., Culver, J.P., Mandeville, J.B., Boas, D.A., 2003. Temporal comparison of functional brain imaging with diffuse optical tomography and fMRI during rat forepaw stimulation. *Phys. Med. Biol.* 48 (10), 1391.

- Smith, A.T., Singh, K.D., Greenlee, M.W., 2000. Attentional suppression of activity in the human visual cortex. *Neuroreport* 11 (2), 271–278.
- Smith, A.T., Williams, A.L., Singh, K.D., 2004. Negative BOLD in the visual cortex: evidence against blood stealing. *Hum. Brain Mapp.* 21 (4), 213–220.
- Stefanovic, B., Wernking, J.M., Pike, G.B., 2004. Hemodynamic and metabolic responses to neuronal inhibition. *NeuroImage* 22 (2), 771–778.
- Strangman, G., Culver, J.P., Thompson, J.H., Boas, D.A., 2002. A quantitative comparison of simultaneous BOLD fMRI and NIRS recordings during functional brain activation. *NeuroImage* 17 (2), 719–731.
- Tana, M.G., Sclocco, R., Bianchi, A.M., 2012. GMAC: a Matlab toolbox for spectral granger causality analysis of fMRI data. *Comput. Biol. Med.* 42, 943–956.
- Tootell, R.B., Mendola, J.D., Hadjikhani, N.K., Liu, A.K., Dale, A.M., 1998. The representation of the ipsilateral visual field in human cerebral cortex. *Proc. Natl. Acad. Sci. U. S. A.* 95 (3), 818–824.
- Toronov, V., Walker, S., Gupta, R., Choi, J.H., Gratton, E., Hueber, D., Webb, A., 2003. The roles of changes in deoxyhemoglobin concentration and regional cerebral blood volume in the fMRI BOLD signal. *NeuroImage* 19 (4), 1521–1531.
- Toronov, V.Y., Zhang, X., Webb, A.G., 2006. Group Analysis of FMRI and NIR data Simultaneously Acquired During Visual Stimulation in Humans (61630S–61630S–9).
- Wade, A.R., 2002. The negative BOLD signal unmasked. *Neuron* 36 (6), 993–995.
- Watanabe, H., Homae, F., Taga, G., 2012. Activation and deactivation in response to visual stimulation in the occipital cortex of 6-month-old human infants. *Dev. Psychobiol.* 54 (1), 1–15.